DEUTSCHES ELEKTRONEN-SYNCHROTRON DESY

DESY SR-71/6
November 1971

Anisotropy of the Dielectric Constants of Trigonal Selenium and Tellurium Between 3 eV and 30 eV

by

P. Bammes, R. Klucker, and E. E. Koch
Sektion Physik der Universität München

and

T. Tuomi
Deutsches Elektronen-Synchrotron DESY, Hamburg

2 HAMBURG 52 · NOTKESTIEG 1

To be sure that your preprints are promptly included in the HIGH ENERGY PHYSICS INDEX, send them to the following address (if possible by air mail):

DESY
Bibliothek
2 Hamburg 52
Notkestieg 1
Germany

Anisotropy of the Dielectric Constants of Trigonal Selenium and Tellurium between 3 eV and 30 eV[≠]

P. Bammes, R. Knucker, and E. E. Koch
Sektion Physik der Universität München, München, Germany

and

T. Tuomi[+]
Deutsches Elektronen-Synchrotron DESY, Hamburg, Germany

[≠] Supported by the Deutsche Forschungsgemeinschaft

[+] Alexander von Humboldt Foundation Fellow on leave from the Helsinki University of Technology

The reflectivity of Se and Te Single crystals has been measured at near normal incidence for photon energies between 3 and 30 eV with the electric field vector lying parallel and perpendicular to the c-axis of the crystals. The measurements were taken using the polarized continuum of the synchrotron radiation of DESY. A Kramers-Kronig analysis gave the optical constants for both directions of polarization. For both substances electron energy loss measurements are reported. Comparison to the optical data gives satisfactory agreement. Even at high energies we observe considerable anisotropic behaviour and several new spectral features. They are discussed in terms of recent band structure calculations.

Die Reflektivität von Se und Te Einkristallen wurde für Photonenenergien zwischen 3 und 30 eV bei nahezu senkrechtem Einfall mit dem elektrischen Feldvektor parallel und senkrecht zur c-Achse der Kristalle gemessen. Für diese Experimente wurde das polarisierte Kontinuum der Synchrotronstrahlung von DESY benutzt. Eine Kramers-Kronig Analyse lieferte die optischen Konstanten für beide Polarisationsrichtungen. Für beide Substanzen wird über Elektronenenergieverlustmessungen berichtet. Der Vergleich mit den optischen Daten ergibt eine befriedigende Übereinstimmung. Auch bei hohen Energien beobachten wir für beide Substanzen ein beträchtliches anisotropes Verhalten und mehrere neue Strukturen. Sie werden an Hand von neuen Bandstruktur-Rechnungen diskutiert.

I. INTRODUCTION

Considerable spectroscopic information on the electronic excitations and their anisotropic behaviour in trigonal selenium and tellurium in the fundamental absorption region has been obtained so far [1, 2]. Due to the lack of suitable polarizers for the far vacuum ultraviolet, measurements with linearly polarized light have been limited to photon energies smaller than about 12 eV. For Se this problem has been overcome by measuring the reflectance of unpolarized light from two different crystal planes with the c-axis parallel ($\parallel$) and perpendicular ($\perp$) to the reflecting surface [3]. The anisotropy has then been calculated from these measurements.

Electron energy loss experiments, for which there are not such severe problems concerning the energy range, have been performed for both, Se and Te [4, 5]. However, the anisotropic behaviour has not been investigated in these experiments.

Here we report on measurements of the reflectance of trigonal Se and Te single crystals for photon energies from 3 eV to 30 eV from which the anisotropic optical constants are deduced. In the same energy range the dependence of the structure of the electron energy loss function on the momentum transfer $\hbar\underline{k}$ to the crystal has been studied. The results of both experiments are compared and discussed with the help of recent band structure calculations.

2. EXPERIMENTS

2.1 Reflection measurements

For the optical experiments we have used the polarized continuum of the synchrotron radiation of the 7.5 GeV Electron-Synchrotron DESY [6, 7]. The radiation was monochromatized by a near normal incidence monochromator in a modified Wadsworth mount [8]. Advantage was taken of a dispersion plane perpendicular to the plane of the synchrotron [9]. Figure 1 gives a sketch of the experimental arrangement. The pre-mirror reflects the light emitted by the electrons in the synchrotron orbit to the monochromator. The electric field vector $\underline{E}$ of the synchrotron radiation lies perpendicular to the plane of the drawing. Since the plane of incidence of the pre-mirror as well as that of the grating are perpendicular to $\underline{E}$ this arrangement produces an even higher degree of polarization as compared to that of the incident synchrotron radiation. The degree of polarization as given by $(I_{\parallel} - I_{\perp})/(I_{\parallel} + I_{\perp})$ was estimated to be better than 0.94. Here $I_{\parallel}$ and $I_{\perp}$ are the intensities of the light components polarized parallel ($\parallel$) and perpendicular ($\perp$) to the electron orbit respectively.

In the reflectometer sample and detector could be rotated independently [10]. This allowed the spectra to be taken at various angles of incidence. Moreover, the sample and the detector could be rotated around the optical axis, which made it possible to measure spectra with light polarized parallel and perpendicular to the c-axis of the crystals.

Depending on the energy range different gratings, filters and detectors were used: for energies up to 20 eV we used a 600 lines/mm grating blazed at 1200 Å with an Al + MgF_2 coating, for the range from 10 to 30 eV a 1200 lines/mm grating blazed at 600 Å with an Au coating. With these gratings a spectral resolution of 4 Å and 2 Å respectively was easily obtained.

Quartz, MgF_2, and LiF were used as filters for measurements up to 7.0, 10.5, and 11.5 eV respectively. A Sodiumsalicylate coated photomultiplier (EMI model 9781 B) served as a detector for photon energies up to 12 eV. For photon energies from 7 to 30 eV spectra were obtained with an open magnetic multiplier (Bendix model 306). These techniques were employed in order to have optimum intensity for a particular wavelength range free from higher spectral orders and straylight. The measurements were performed at room temperature with crystals grown from the melt, the c-axis of the crystals lying parallel to the surface. The crystals were freshly cleaved before they were mounted into the sample holder. The direction of the c-axis within the surface was determined by X-ray diffraction.

In contrast to the relative spectral shape the absolute value of the reflectance was not determined with great accuracy since the reflected intensity I_r and the incident intensity I_o were not measured simultaneously.

When the reflectance curves were drawn, different overlapping parts of the spectra, measured with different gratings and/or filters and detectors, had to be adjusted to each other. Finally, to bring the relative reflection spectra to absolute values we normalized our measurements between 3.5 eV and 6 eV to the spectra taken by Henrion [11] and Leiga [3] for Se and Tutihasi, Roberts, Keezer and Drews [2] for Te. Because this procedure introduces some ambiguity, the absolute values given have to be taken with some reservation.

2.2 Electron energy loss measurements

The electron energy loss spectra were measured with single-crystal Se and Te films approximately 1000 Å thick. Se of 99.999 % purity was evaporated onto $10\bar{1}0$-faces of Te crystals as thin films [12]. The films were prepared selfsupporting on apertures. The preparation of the Te-samples will be described elsewhere [13]. The structure of the samples was checked by electron diffraction patterns. The c-axis was lying in the plane of the crystals.

Energy losses of 30 keV electrons traversing the films were measured with a Möllenstedt-type analyzer [14, 15]. Spectra for various scattering angles ϑ and φ (declination and azimuth) could be taken without mechanical adjustments by electrostatic bending of the electron beam. This allowed for detection of even small anisotropic effects. In order to have as much intensity as possible, a comparitively low resolution of 1 eV was used.

The direction of the scattered electrons was accurate within $\pm 1.5 \times 10^{-4}$ rad and $\pm 9^{\circ}$ for the angle of declination ϑ and the azimuth φ respectively (Fig. 2). Spectra were taken for $\vartheta = 1 \times 10^{-3}$ rad. For this angle the direction of the momentum transfer $\not\Delta \underline{k}$ is defined with a maximal halfwidth of 4°. However, this direction is not perpendicular to the electron beam and changes with energy loss [16, 17]. In order to have this direction as close as possible parallel to the foil for spectra $\underline{k} \parallel \underline{c}$ the sample was titled at an angle of 12° as shown in Fig. 2. This minimized the angle at which $\underline{k}$ was outside the plane (maximal deviation from the plane 7°) and made the necessary correction for obtaining $|\mathrm{Im}\, \hat{\varepsilon}^{-1}|$ from the experimental data as small as possible. For the case $\underline{k} \perp \underline{c}$ titling is not necessary.

3. RESULTS AND DISCUSSION

3.1 Optical experiment

In Fig. 3 the reflectance spectra of Se and Te for an angle of incidence of 15^0 are given. Below 3 eV measurements of Ref. 2, and Ref. 11 are included as well as our extrapolation to 0 eV. The reflectance values at 0 eV were calculated from the dielectric constant ε for small energies taken from Gobrecht and Tausend [18] for Se ($\varepsilon_1^{\parallel} = 13.3$ and $\varepsilon_1^{\perp} = 9.0$) and Geick, Grosse and Richter [19] for Te ($\varepsilon_1^{\parallel} = 36$ and $\varepsilon_1^{\perp} = 23$). Our spectra were measured for $\underline{E} \parallel \underline{c}$ with $\underline{E}$ lying perpendicular to the plane of incidence and for $\underline{E} \perp \underline{c}$ with $\underline{E}$ lying parallel to the plane of incidence.

In the range from 3 eV to 6 eV we observe a prominent reflectance maximum followed by a sharp decrease of the reflectance for both substances and both directions of polarization. In the range from 6 eV up to approximately 11 eV strong anisotropic behaviour is found. Up to this photon energy our measurements agree fairly well with earlier results. At higher energies the spectra show two pronounced structures at around 14 eV for both directions of polarization, followed by a smooth decrease of the reflectance. The energies for the peaks observed in the reflectance are listed in Table 1.

In order to obtain the complex dielectric constant $\hat{\varepsilon}(\hbar\omega) = \varepsilon_1(\hbar\omega) + i\,\varepsilon_2(\hbar\omega)$ a Kramers-Kronig transformation was applied to the reflectivity spectra $R(\hbar\omega)$ of Fig. 2 for both directions of polarization. A computer program gave ε_1, ε_2 and the energy loss function $|\mathrm{Im}\,\hat{\varepsilon}^{-1}|$. It was capable of dealing with reflectance data taken at non-normal incidence and with the $\underline{E}$ vector parallel and perpendicular to the plane of incidence [20]. Our ε_1 and ε_2 curves for both materials for $\underline{E} \parallel \underline{c}$ and $\underline{E} \perp \underline{c}$ are shown in Figs. 4 and 5. Because of possible errors in the absolute reflectivity and the extrapolation for the energy ranges not covered by the experiment the computed absolute values for

ε_1 and ε_2 are not expected to be very accurate, the position and shape of the peaks, however, as well as their relative heights should be fairly correct.

It is worth noting, that at about 9 eV for Se and at about 6 eV for Te the imaginary part of the dielectric constant ε_2 for $\underline{E} \perp \underline{c}$ becomes larger and stays larger with increasing photon energy than ε_2 for $\underline{E} \parallel \underline{c}$.

In Fig. 6 the energy loss functions $|\mathrm{Im}\,\hat{\varepsilon}^{-1}|$ derived from the optically determined constants ε_1 and ε_2 are shown. This quantity can be directly compared with that obtained from electron energy loss experiments.

3.2 Electron energy loss experiments

The only electron energy loss that has to be considered is the single volume loss, since the only detectable multiple volume loss has its maximum outside the spectral range investigated. The cross section for the surface losses at $\vartheta = 1 \cdot 10^{-3}$ rad is so small that it may be neglected. For the single volume loss the experimental spectrum $S(\hbar\omega)$ is given as [21] :

$$S_{\parallel,\perp}(\hbar\omega,\vartheta)\,d\hbar\omega\,d\Omega \propto (\vartheta^2+\vartheta_E^2)^{-1} \cdot \mathrm{Im}\;\hat{\varepsilon}_{\parallel,\perp}^{-1}\;\; d\hbar\omega\,d\Omega$$

($\vartheta_E = \hbar\omega/2\,E_0$, E_0 energy of the incident electrons, $d\Omega$ solid angle).

In Fig. 7 $|\mathrm{Im}\,\hat{\varepsilon}^{-1}|$ determined from $S(\hbar\omega,\vartheta)$ for both directions of polarization is shown. The correction by the factor $(\vartheta^2+\vartheta_E^2)$ changes with energy loss from 0.9 to 1.15 and gives a relevant contribution only for energies exceeding 20 eV. The convolutions by the experimental spread in energy and angle are negligible. Note, that in this experiment the ratio of $|\mathrm{Im}\,\hat{\varepsilon}^{-1}|$ for $\underline{k} \parallel \underline{c}$ to $|\mathrm{Im}\,\hat{\varepsilon}^{-1}|$ for $\underline{k} \perp \underline{c}$ is directly determined by the measurements.

Spectra from several samples showed a good reproducibility. Minor deviations could be observed, however, between freshly

prepared films and those which were older. This aging effect is more pronounced for Te than for Se. We display here spectra obtained from the older samples, because the deviations are probably due to annealing processes.

The energy loss spectra for both substances show a strong maximum with smaller structures on both slopes. The main peak may be interpreted as due to the collective oscillation of the 6 outer s- and p-electrons. The calculated plasmafrequency $\omega_p = (4\pi ne^2/m)^{1/2}$ has in both cases a value smaller by approximately 10 % than the experimentally observed peak positions. The single excitations at lower energies from which the longitudinal modes are observed in the loss spectra, are the main cause of the partially anisotropic shift of the plasmafrequency to higher energies.

3.3 Comparison of optical and electron loss experiments

We are going to compare $|\mathrm{Im}\,\hat{\varepsilon}^{-1}|$ for both directions of polarization, each independently determined by optical and electron loss experiments (Fig. 6, 7).

For Se we obtain a very similar anisotropic behaviour of the $|\mathrm{Im}\,\hat{\varepsilon}^{-1}|$ curves from both methods: below approximately 7 eV $|\mathrm{Im}\,\hat{\varepsilon}_{\perp}^{-1}|$ is larger than $|\mathrm{Im}\,\hat{\varepsilon}_{\parallel}^{-1}|$, between 7 eV and 20 eV $|\mathrm{Im}\,\varepsilon_{\parallel}^{-1}|$ is larger and becomes smaller again for energies exceeding 20 eV. Both measurements show maxima at 6 eV ($\perp$ c) and 11 eV ($\parallel$ c) followed by a large maximum at 19.0 eV ($\parallel$ c) and 20.3 eV ($\perp$ c) respectively.

However, some discrepancies are worth noting: whereas the optical experiments give more structured curves for energies below 15 eV the energy loss esperiments show some additional structure for energies exceeding 20 eV. Moreover, the amount of anisotropy is larger for the optical curves.

For the range 0 - 15 eV the spread in energy and angle for the energy loss data cannot explain the discrepancy. Also the reduction of the optical data as described in 2.1. and possible errors introduced by the Kramers-Kronig analysis can be excluded as sources of these differences.

Two reasons may cause the observed differences: 1. We used differently prepared samples in both experiments, 2. In electron loss experiments the optical constants depend on $\underline{k}$. This spatial dispersion [22] may cause a structure, different from the one observed in the optical experiment. Since the special experimental set-up, as described above, gives momentum transfer of approximately 15 % of the maximum $\underline{k}$ possible within the boundary of the Brillouin zone, no direct band to band transitions are observed. This is equivalent to a horizontal shift of the energy bands with respect to each other [22].

For Te the differences may be explained by the same arguments. It is remarkable, that $|\mathrm{Im}\,\hat{\varepsilon}_{\perp}^{-1}|$ is larger than $|\mathrm{Im}\,\hat{\varepsilon}_{\parallel}^{-1}|$ for the spectral range shown in Fig. 7. If the sum rule

$$-\int_0^\infty \mathrm{Im}\,\hat{\varepsilon}_{\perp,\parallel}^{-1}\,(\omega')\,\omega'\,d\omega' = 2\pi\omega_p^2$$

is taken into account, one has to expect, that $|\mathrm{Im}\,\hat{\varepsilon}_{\perp}^{-1}|$ becomes smaller than $|\mathrm{Im}\,\hat{\varepsilon}_{\parallel}^{-1}|$ at higher energies. Concerning the structure the results from both experiments are very similar. Both methods yield maxima at 5 eV ($\perp$ c) and at about 17.3 eV ($\parallel$ c and $\perp$ c). Further the position of the shoulders at 8 eV ($\parallel$ c), 11.5 eV ($\parallel$ c) and 12 eV ($\perp$ c) show a good agreement.

4. COMPARISON WITH BAND STRUCTURE CALCULATIONS

4.1 Selenium

Our results for Se are compared with the calculated electron energy bands. A part of the band structure due to Sandrock [23] is shown in Fig. 8. He discusses transitions extending up to 12 eV. The spectral features in the energy range from 0 to 6 eV are due to excitations of electrons from the upper part of the valence band to the lower part of the conduction band. The main contribution to the ε_2 spectra in the range 7 eV to 9 eV originates from transitions from the lower valence band to the lower conduction band triplet as well as from the upper valence band to the upper conduction band triplet.

As the new results of this work show, there is still a relatively large contribution to the ε_2-spectrum for energies exceeding 12 eV. There are peaks centered at 12.3 eV for both directions of polarization. The band structure of Fig. 8 suggests that they may be associated with transitions from the lower valence to the upper conduction band triplet.

For both directions of polarization we observe weak reflectance peaks at about 16.5 eV. The corresponding structures are not well discernible in the ε_2-curves. However, in the $|\mathrm{Im}\,\hat{\varepsilon}^{-1}|$ curves, as obtained from both methods (Figs. 6, 7) they can be distinguished as shoulders. Since for higher energies $|\mathrm{Im}\,\hat{\varepsilon}^{-1}| \approx \varepsilon_2$ whereas for smaller energies $|\mathrm{Im}\,\hat{\varepsilon}^{-1}| \ll \varepsilon_2$ holds, this small ε_2 structures do show up more clearly in the $|\mathrm{Im}\,\hat{\varepsilon}^{-1}|$ curves. Sandrock [23] gives the eigenvalues at symmetry points for three more valence bands (s-type) below the lower valence band triplet. Transitions from these bands, not included in Fig. 8, should occur in the energy range from 16 eV to 25 eV. We, therefore, consider the observed structures above 16 eV as due to such transitions.

The next higher transitions in Se are those from the 3d-core level to the conduction band which do not "switch on" until about 55 eV as seen in the energy loss spectrum not displayed here.

4.2 Tellurium

A similar kind of analysis as for Se can be made for Te. The most recent one of a number of electron energy band calculations was made by Maschke [24] using the pseudopotential method. A part of this band structure is shown in Fig. 9. The ε_2-spectra for the two directions of polarization up to 11 eV are rather satisfactorely interpreted, as discussed by Maschke, in terms of electronic transitions from the six mostly p-type valence bands to the six conduction bands shown in Fig. 9. As in the case of Se the six valence bands as well as the six conduction bands consist of two triplets.

A contribution from a third valence band triplet to the lower conduction bands will possibly show up in the region near 10 eV. This triplet, not shown in Fig. 9, originates from the atomic s-states and lies about 10 eV below the lower conduction band triplet [25]. The maxima at about 12 eV, seen in the ε_2-spectra (Fig. 5) may well be due to the transitions from this s-type valence band triplet to the lower conduction band triplet. The next maxima at approximately 16 eV in the reflectance spectra, which appear as shoulders in the ε_2-curves, may be mainly attributed to the transitions from the s-type valence band to the upper conduction band triplet.

The next deeper levels below the s-type valence bands lie about 40 eV below the lower conduction band triplet. Transitions from these atomic 4d core levels to the conduction band thus fall outside the photon energy range investigated in this work.

A more detailed assignment to special points within the brillouin-zone is not possible for both, Se and Te, since for both substances the contribution to the ε_2-spectra originate from rather large regions of the k-space [23, 24, 25].

Acknowledgement

This work is the result of the cooperation of several groups. While the optical measurements have been performed at the Deutsches Elektronen-Synchrotron by three of us (R.K., E.E.K. and T.T.) the electron energy loss experiment has been carried out at the Universität München by P.B. We are grateful to the staff of the synchrotron radiation group at DESY for technical assistance. In the early stage of the optical experiment B. Gotchev kindly assisted us. Thanks are also due to O. Pilvič and G. Weiser for providing us with single crystals. P.B. wishes to thank C.H. Griffiths for advice in preparing the Se films.

We are grateful to A. Otto, M. Skibowski and W. Steinmann for criticism and discussions. We are especially indebted to K. Maschke for discussions and making his band structure calculations available to us prior to publication.

References

1. E. Mohler, J. Stuke, and G. Zimmerer, phys.stat.sol. 22, K 49 (1967)

2. H. Merdy, Thèse, Faculté des Sciences de l'Université de Dakar (1965)
   S. Tutihasi, G.G. Roberts, R.C. Keezer, and R.E. Drews, Phys.Rev. 177, 1143 (1969) and references given in that paper

3. A.G. Leiga, J. Appl.Phys. 39, 2149 (1968)

   A.G. Leiga, J. Opt.Soc.Am. 58, 880 (1968)

4. H. Friedmann, Z. Naturf. 11a, 373 (1956)

5. J.D. Robins, Proc.Phys.Soc. 79, 119 (1962) and references given in that paper

6. R. Haensel and C. Kunz, Z. Angew. Phys. 23, 276 (1967)

7. R.P. Godwin in Springer Tracts in Modern Physics Vol. 51, p.1, ed. by G. Höhler, Springer, Berlin 1969

8. M. Skibowski and W. Steinmann, J.Opt.Soc.Am. 57, 112 (1967)

9. E.E. Koch and M. Skibowski, Chem.Phys. Letters 9, 429 (1971)

10. B. Feuerbacher, M. Skibowski, and R.P. Godwin, Rev.Sci.Instr. 40, 305 (1969)

11. W. Henrion, phys.stat.sol. 22, K 33 (1967)

12. C.H. Griffiths and H. Sang, Appl.Phys. Letters 11, 118 (1967)

13. P. Bammes, A. Otto and [illegible]

14. G. Möllenstedt, Optik 5, 499 (1949)

15. J.B. Swan, A. Otto, and H. Fellenzer, phys.stat.sol. 23, 171 (1967)

16. K. Zeppenfeld, Z. Physik 211, 391 (1968)

17. S. Kunstreich and A. Otto, Opt.Comm. 1, 45 (1969)

18. H. Gobrecht and A. Tausend, Z. Physik 161, 205 (1961)

19. R. Geick, P. Grosse, and W. Richter in: The Physics of Selenium and Tellurium ed. by W.C. Cooper, Pergamon Press, New York, 1969, p.309

20 R. Klucker, unpublished

21. R.H. Ritchie, Phys.Rev. 106, 874 (1957)

22. K. Zeppenfeld, Opt.Comm. 1, 119 (1969)

23. R. Sandrock, Phys.Rev. 169, 642 (1968)

R. Sandrock, phys.stat.sol. (b) 43, 199 (1971) and references given therin

24. K. Maschke, phys.stat.sol., to be published (Oct. 71) and references given therin

25. K. Maschke, private communication

Table I

Energy position (in eV) of the most prominent structures of the 15° reflectance spectra for Se and Te single crystals for both directions of polarisation. Shoulders are denoted by sh. Values below 3 eV are taken from Refs. [2, 11].

Se		Te	
$\underline{E} \parallel \underline{c}$	$\underline{E} \perp \underline{c}$	$\underline{E} \parallel \underline{c}$	$\underline{E} \perp \underline{c}$
2.0	1.9	1.0	1.0
3.1	3.1 sh	1.4	
4.0	3.9	2.4	2.4
4.9 sh	4.8 sh	2.9	
6.7 sh	6.8 sh	3.4 sh	3.6 sh
7.5	7.4 sh	5.4 sh	
8.6 sh		7.4	
9.1	8.9	8.0 sh	8.0
10.4 sh	10.5	9.5	9.2
13.0	13.5	11.2 sh	10.9 sh
16.2	16.4	12.9	13.2
		16.3	15.9
			16.6

Figure captions

Fig. 1 Experimental arrangement for the optical experiment.

Fig. 2 $\underline{k}$ - directions relative to the crystal in the electron loss experiment. 2a) The plane of the incident and scattered electron beam for $\underline{k} \parallel \underline{c}$ and $\underline{k} \perp \underline{c}$. The change of the $\underline{k}$ - direction with loss energy is described. 2b) The plane of the crystal for $\underline{k} \parallel \underline{c}$ and $\underline{k} \perp \underline{c}$. The incident electron beam is perpendicular to the drawing. The uncertainty of the $\underline{k}$ - direction (φ) within the crystal plane is described (the broken vectors indicate the angular half width).

Fig. 3 Reflectance of Se and Te single crystals for an angle of incidence of 15° with $\underline{E} \parallel \underline{c}$ (solid line) and $\underline{E} \perp \underline{c}$ (broken line). Below 3 eV measurements of Ref. [2] and Ref. [11] are included.

Fig. 4 Dielectric constant ε_1 for Se and Te for $\underline{E} \parallel \underline{c}$ (solid line) and $\underline{E} \perp \underline{c}$ (broken line).

Fig. 5 Dielectric constant ε_2 for Se and Te for $\underline{E} \parallel \underline{c}$ (solid line) and $\underline{E} \perp \underline{c}$ (broken line).

Fig. 6 Energy loss function $|\mathrm{Im}\,\hat{\varepsilon}^{-1}|$ for Se and Te for $\underline{E} \parallel \underline{c}$ (solid line) and $\underline{E} \perp \underline{c}$ (broken line) as obtained from the optical data.

Fig. 7 Energy loss function $|\mathrm{Im}\,\hat{\varepsilon}^{-1}|$ for Se and Te for $\underline{k} \parallel \underline{c}$ (solid line) and $\underline{k} \perp \underline{c}$ (broken line) as obtained from the energy loss experiment.

Fig. 8 Energy bands of trigonal Se according to Sandrock (Ref. 23).

Fig. 9 Energy bands of trigonal Te according to Maschke (Ref. 24).

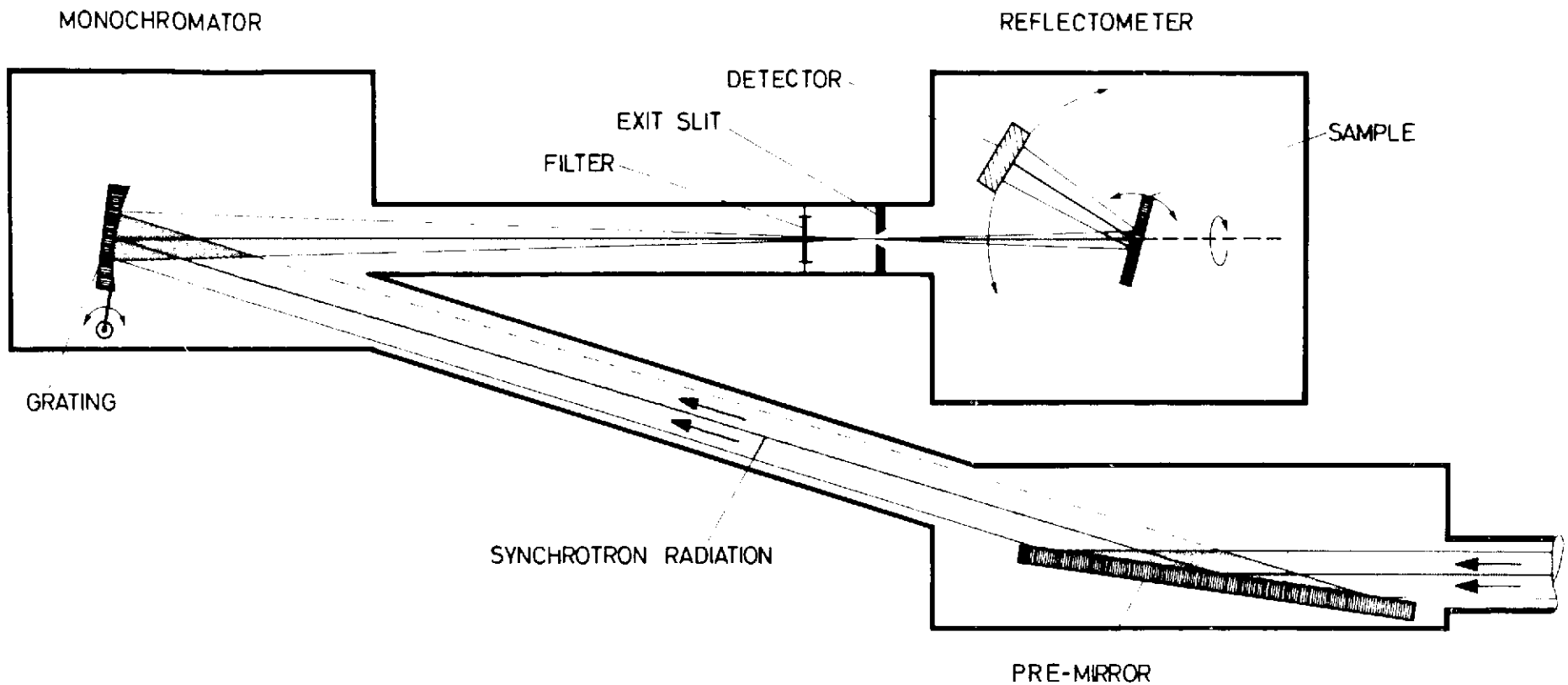
MONOCHROMATOR
REFLECTOMETER
DETECTOR
EXIT SLIT
FILTER
SAMPLE
GRATING
SYNCHROTRON RADIATION
PRE-MIRROR

Fig.1

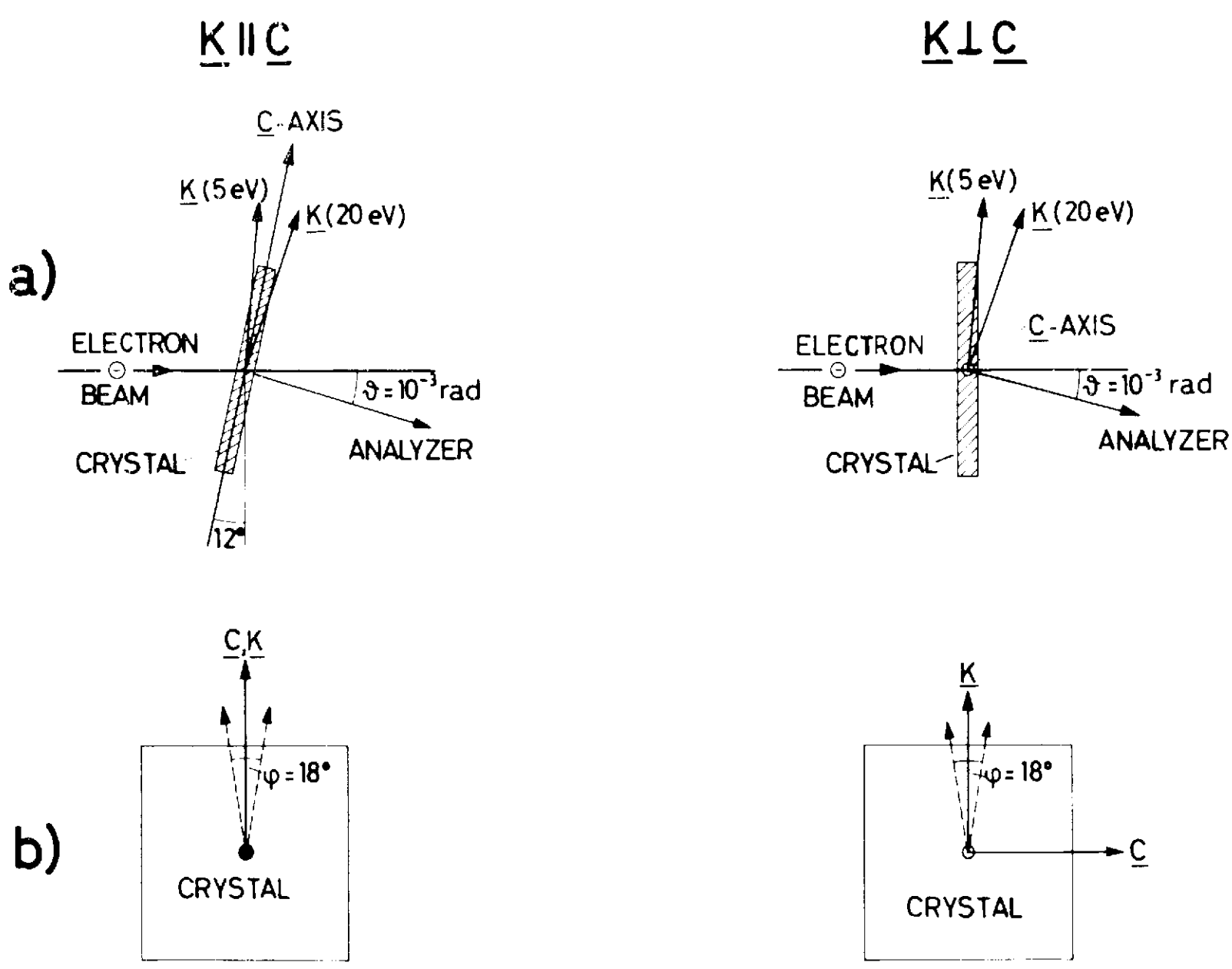
K ∥ C
K ⊥ C
a)
C-AXIS
K(5 eV)
K(20 eV)
ELECTRON
BEAM
CRYSTAL
ANALYZER
ϑ = 10⁻³ rad
12°
b)
C,K
φ = 18°
CRYSTAL
K
C

Fig. 2

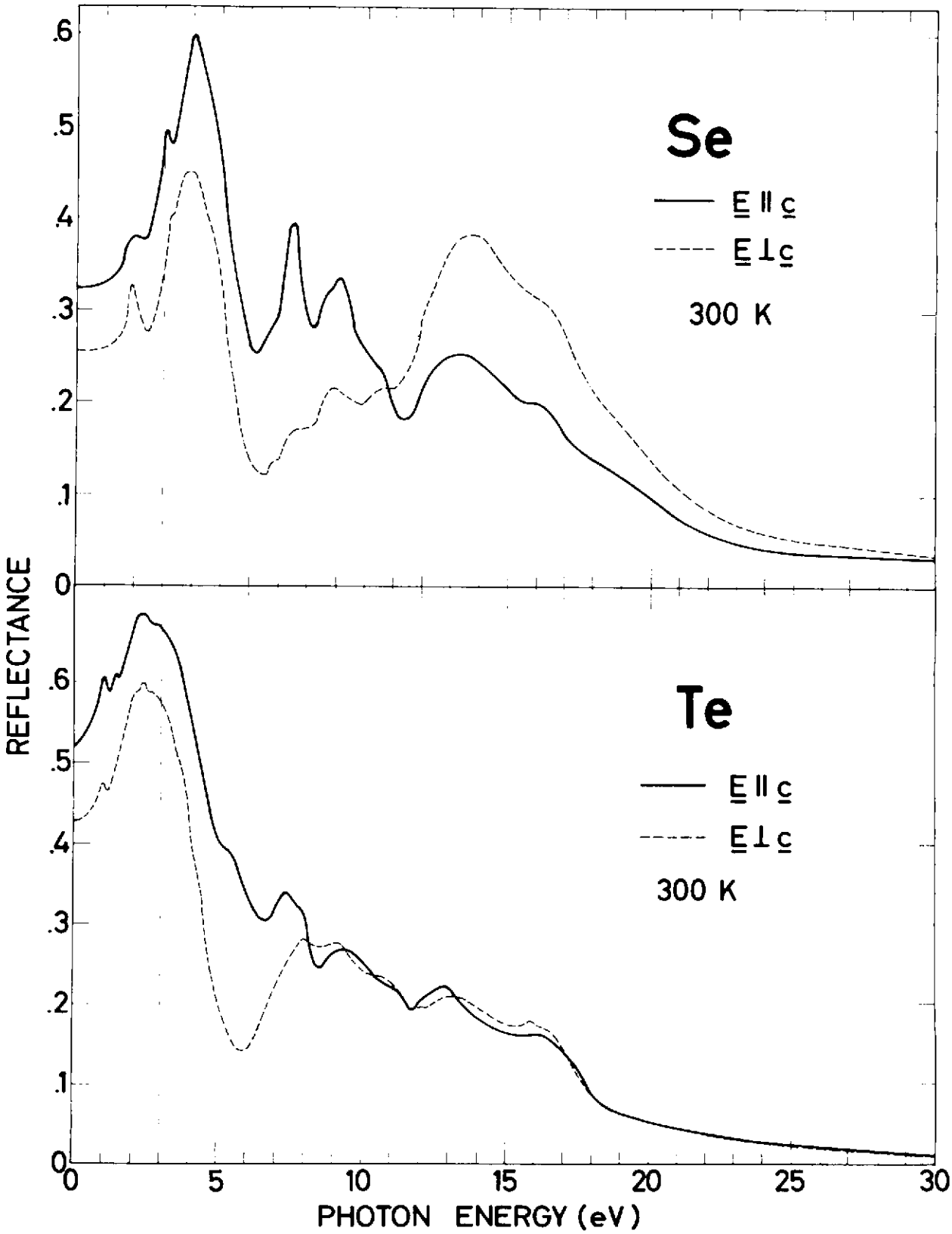
Se
E ∥ c
E ⊥ c
300 K
Te
E ∥ c
E ⊥ c
300 K
REFLECTANCE
PHOTON ENERGY (eV)
0
.1
.2
.3
.4
.5
.6
0
5
10
15
20
25
30

Fig. 3

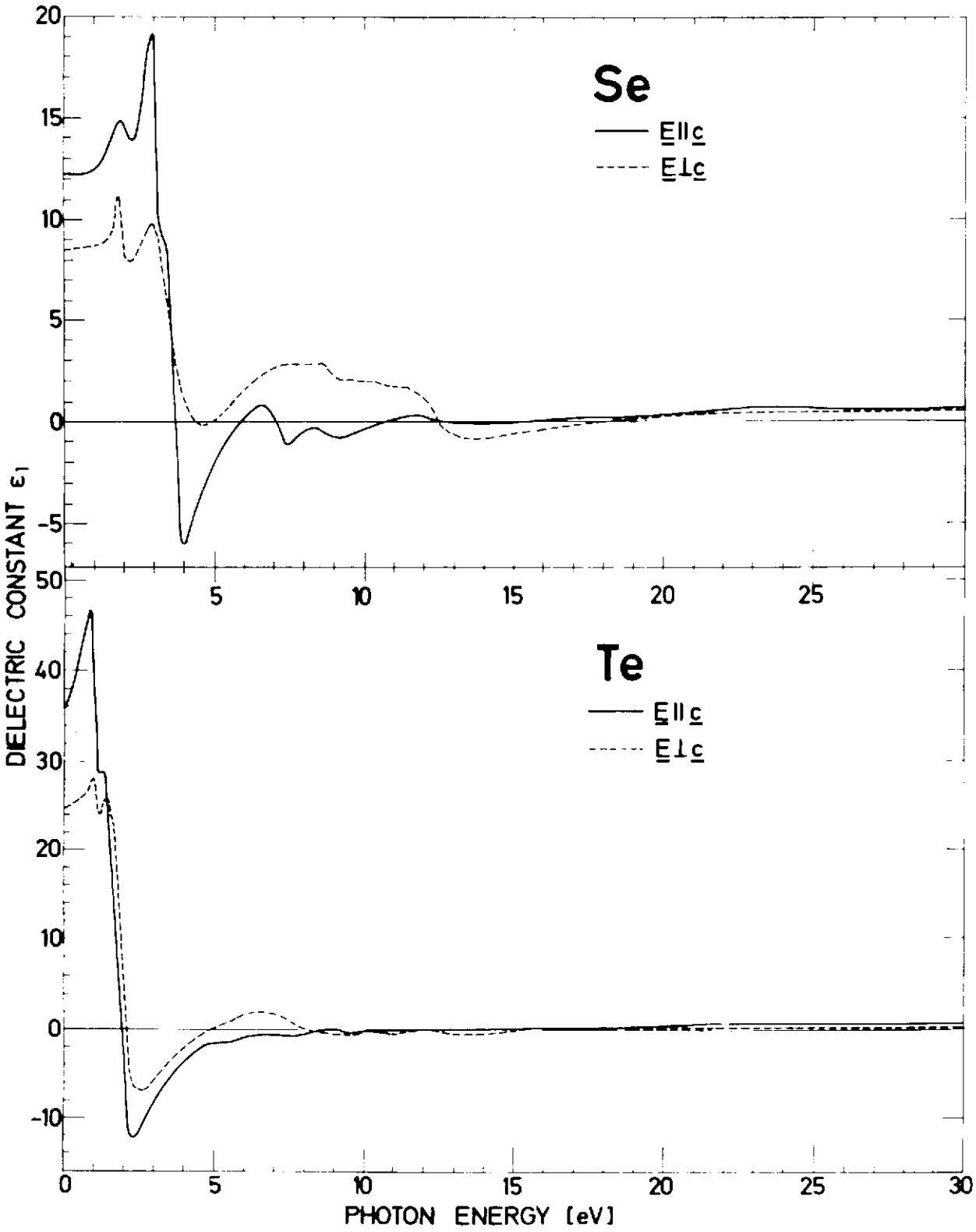
Se
E∥c
E⊥c
Te
E∥c
E⊥c
DIELECTRIC CONSTANT ε1
PHOTON ENERGY [eV]
20
15
10
5
0
-5
50
40
30
20
10
0
-10
0
5
10
15
20
25
30

Fig. 4

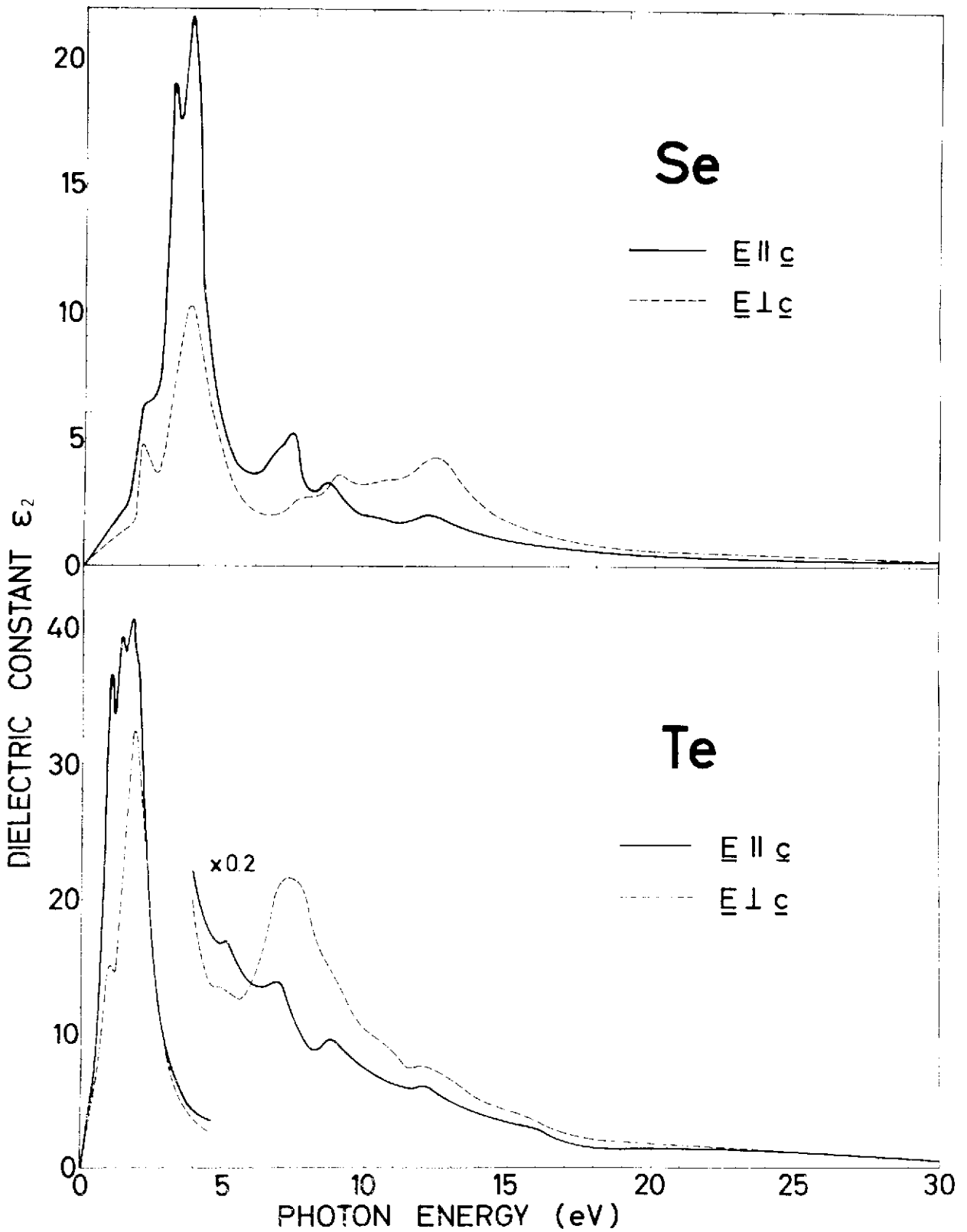
Se
E ∥ c
E ⊥ c
Te
E ∥ c
E ⊥ c
x 0.2
DIELECTRIC CONSTANT ε2
PHOTON ENERGY (eV)
0
5
10
15
20
25
30
40

Fig. 5

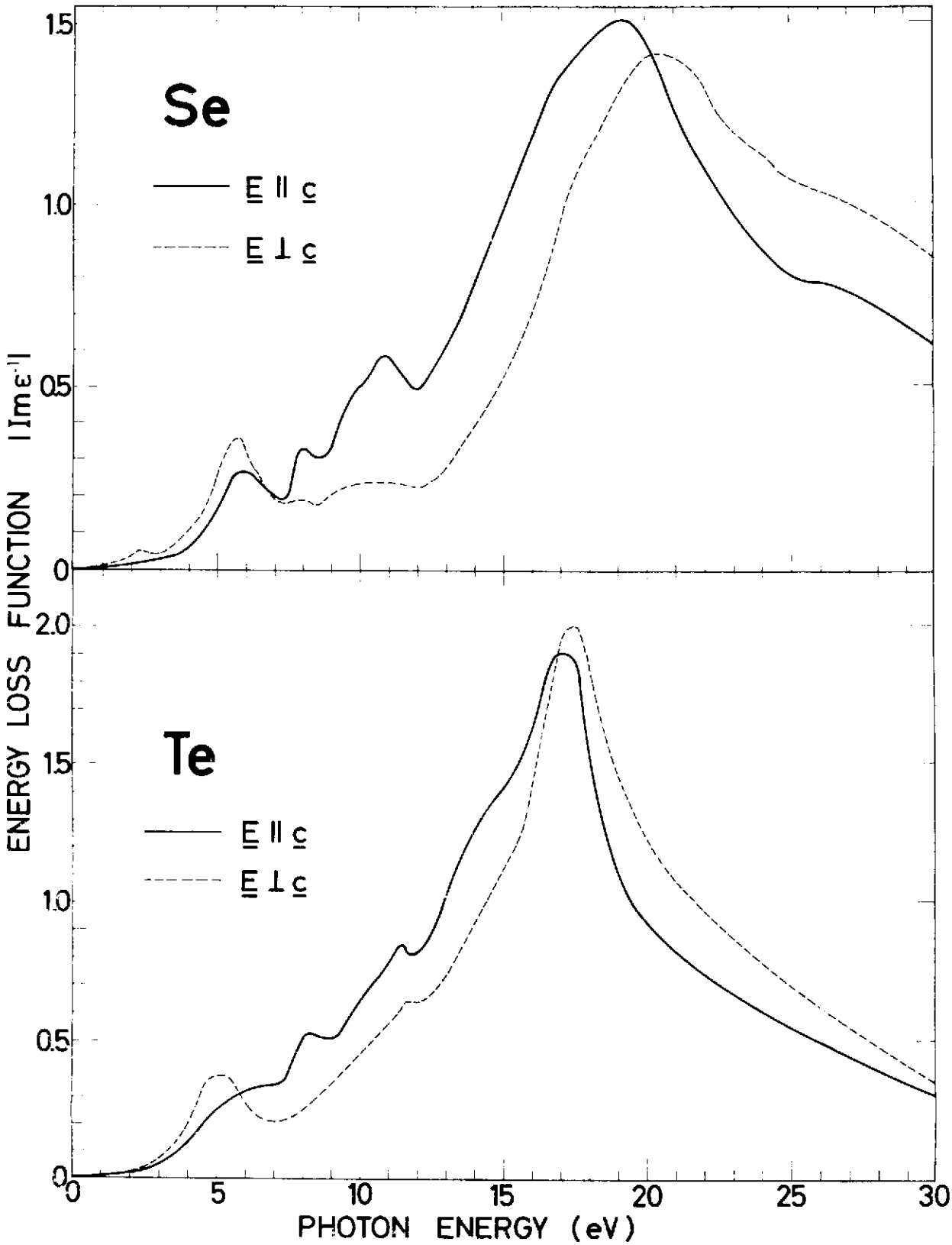
Se
E ∥ c
E ⊥ c
Te
E ∥ c
E ⊥ c
ENERGY LOSS FUNCTION Im ε⁻¹
PHOTON ENERGY (eV)
0
0.5
1.0
1.5
2.0
5
10
15
20
25
30

Fig. 6

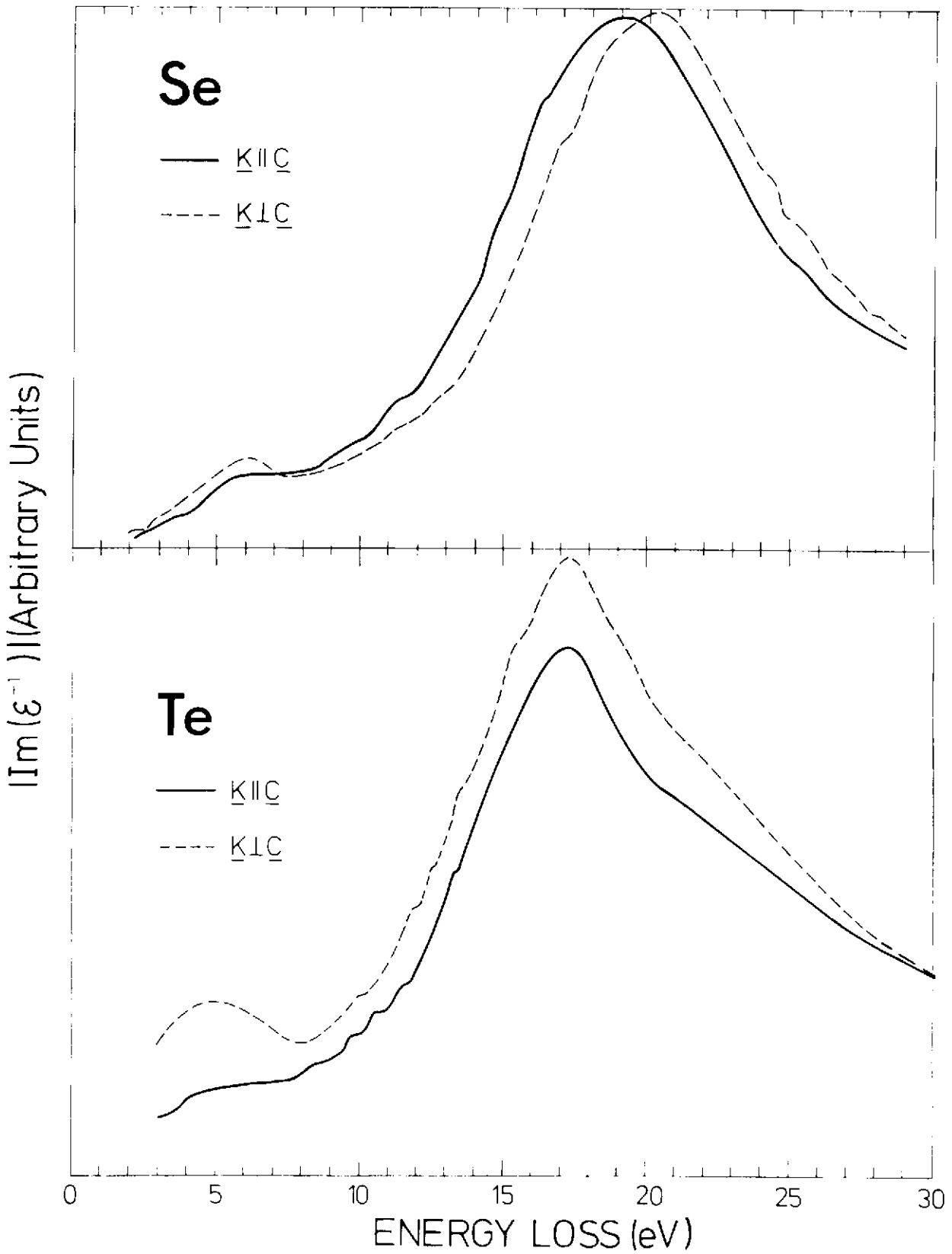
Se
K∥C
K⊥C
Te
K∥C
K⊥C
|Im(ε⁻¹)| (Arbitrary Units)
0
5
10
15
20
25
30
ENERGY LOSS (eV)

Fig. 7

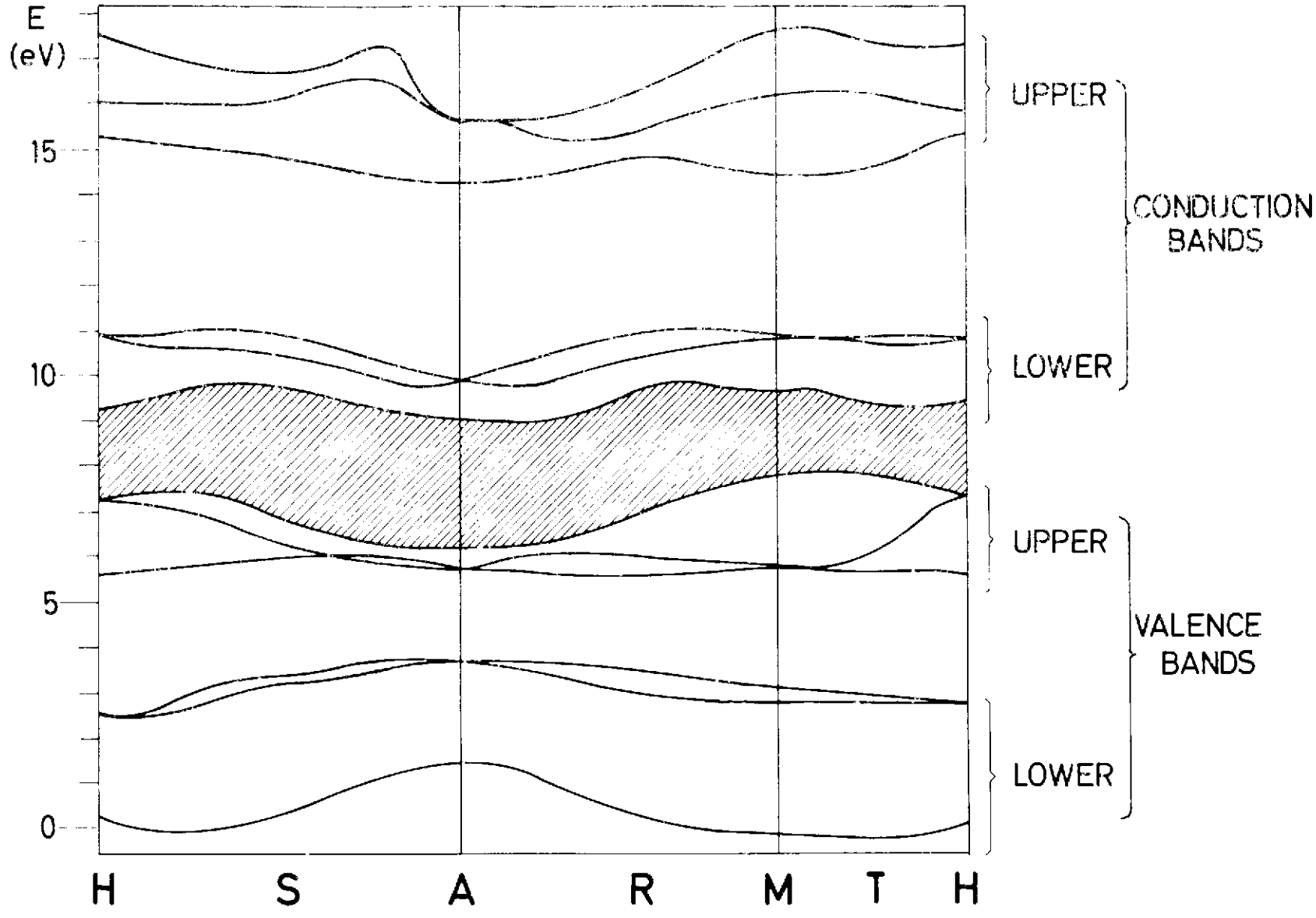

ENERGY BANDS OF TRIGONAL SELENIUM (SANDROCK)

Fig. 8

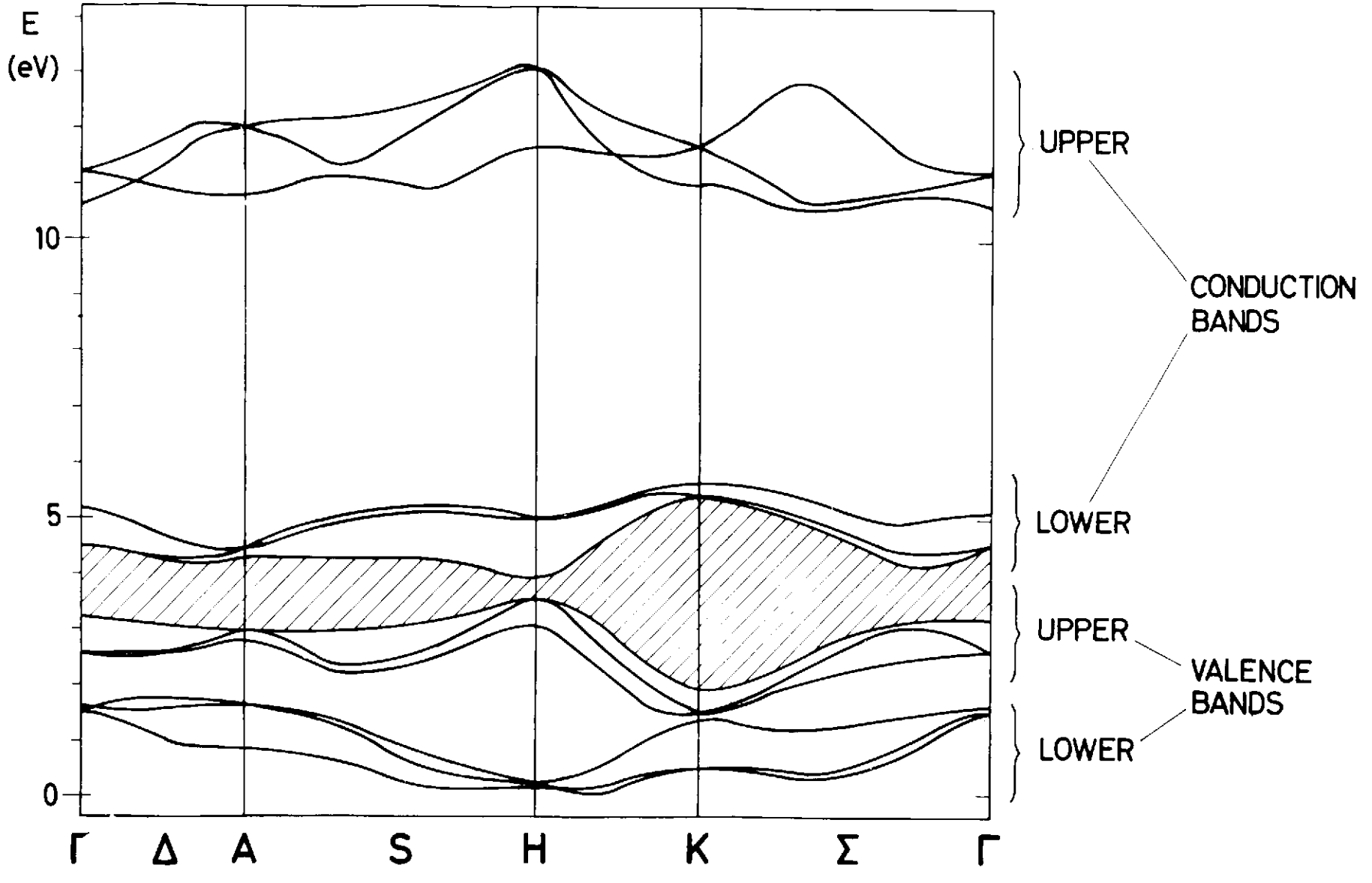

ENERGY BANDS OF TELLURIUM (MASCHKE)

Fig.9